Published in final edited form as:
Wound Repair Regen. 2012 July ; 20(4): 563–572. doi:10.1111/j.1524-475X.2012.00813.x.

Reduction of Burn Progression with Topical Delivery of (Anti-Tumor Necrosis Factor-α)-Hyaluronic Acid Conjugates

Liang Tso Sun, PhD[1], **Emily Friedrich, MS**[1], **Joshua L. Heuslein, BS**[1], **Rachel E. Pferdehirt, BS**[2], **Nicole M. Dangelo, BS**[2], **Shanmugasundaram Natesan, PhD**[3], **Robert J. Christy, PhD**[3], and **Newell R. Washburn, PhD**[1,2,4]

[1]Department of Biomedical Engineering, Carnegie Mellon University, Pittsburgh, Pennsylvania

[2]Department of Chemistry, Carnegie Mellon University, Pittsburgh, Pennsylvania

[3]United States Army Institute for Surgical Research, Fort Sam Houston, Texas

[4]McGowan Institute for Regenerative Medicine, University of Pittsburgh, Pittsburgh, Pennsylvania

Abstract

In this study, we explored whether topical application of antibodies targeting tumor necrosis factor-α (TNF-α) or interleukin-6 (IL-6) conjugated to hyaluronic acid (HA) could reduce the extension of necrosis by modulating inflammation locally in a partial-thickness rat burn model. Partial-thickness to deep partial-thickness burn injuries present significant challenges in healing, as these burns often progress following the initial thermal insult, resulting in necrotic expansion and increased likelihood of secondary complications. Necrotic expansion is driven by a microenvironment with elevated levels of pro-inflammatory mediators, and local neutralization of these using antibody conjugates could reduce burn progression. Trichrome-stained tissue sections indicated the least necrotic tissue in (anti-TNF-α)-HA treated sites, while (anti-IL-6)-HA treated sites displayed similar outcomes to saline controls. This was confirmed by vimentin immunostaining, which demonstrated that HA treatment alone reduced burn progression by nearly 30%, but (anti-TNF-α)-HA reduced it by approximately 70%. At all time points, (anti-TNF-α)-HA treated sites showed reduced tissue levels of IL-1β compared to controls, suggesting inhibition of a downstream mediator of inflammation. Decreased macrophage infiltration in (anti-TNF-α)-HA-treated sites compared to controls was elucidated by immunohistochemical staining of macrophages, suggesting a reduction in overall inflammation in all time points. These results suggest that local targeting of TNF-α may be an effective strategy for preventing progression of partial-thickness burns.

INTRODUCTION

Burns are unique among acute injuries in the progressive nature of tissue necrosis following the initial insult. The initial injury induces a central zone of coagulation, a region of irreversible tissue loss due to protein denaturation and cell death (1). Over the course of several days, the surrounding zone of stasis experiences continuing and potentially irreversible necrotic conversion that expands wound size and depth, leading to delayed healing and increased likelihood of secondary complications and patient morbidity (2, 3). Early interventions to modify the pathophysiological environment, thereby abating tissue

Correspondence and Reprint requests: Newell R. Washburn, PhD, Carnegie Mellon University - Chemistry and Biomedical Engineering, 4400 Fifth Avenue Pittsburgh Pennsylvania 15213, United States, T: 412-268-2130 F: 412-268-6897, washburn@andrew.cmu.edu.

NRW has started a company to commercialize aspects of this research and wishes to disclose a potential conflict of interest.

destruction in the zone of stasis, could potentially reduce the extent of burn injury, and hence offer clinical relevance (4).

Thermal trauma induces significant tissue damage, leading to tissue ischemia, edema and the release of oxidizing agents, which further extend the tissue injury (5). Burned tissue is often described as being in a cytotoxic and degenerative state (6). Several inflammation-mediated mechanisms for continued tissue destruction have been proposed, such as oxidative stress, cell death, hypoperfusion, and vasodilation, leading to tissue ischemia and necrosis (7). Abnormal levels of pro-inflammatory mediators, such as tumor necrosis factor alpha (TNF-α), interleukin-1β (IL-1β), and interleukin-6 (IL-6) have been reported both systemically and locally in burn patients, which suggest these mediators may be centrally involved in establishing the pathophysiological environment of burns.

In this study, we investigated the effects of inhibiting two of these pro-inflammatory mediators: TNF-α and IL-6. TNF-α is known to signal a host of downstream inflammatory mediators, including IL-6 (8), and neutralizing this target could effectively modulate the resultant complex inflammatory cascade. TNF-α activates keratinocytes and macrophages to release reactive oxygen species (ROS), which can induce free radical damages (9–11). Increases in inducible nitric oxide synthase (iNOS), IL-1β, and prostanoids, all downstream effects of TNF-α upregulation, can differentially promote vasodilation or vasoconstrictions (12–14), while TNF-α itself can induce endothelial permeability (15–17). TNF-α-induced prostaglandins can also increase the risk of hypoperfusion in burn wounds (14). Ultimately, these pathological mechanisms may lead to necrotic tissue formation and increase the severity of injury.

In contrast, IL-6 is a pleiotropic cytokine with a broad spectrum of pro- and anti-inflammatory activities in the burn site, also making it a strong candidate for cytokine neutralizing therapy. It is produced by T cells, B cells, monocytes, fibroblasts, keratinocytes, and endothelial cells (18, 19). The general physiological functions of IL-6 are complex; IL-6 induces T-cell proliferation and cytotoxic T-cell differentiation, and terminal macrophage differentiation, making it important in a broad range of inflammatory settings (20). The concentration of circulating IL-6 can be elevated in burn and septic patients 100-fold (21), and it is thought to be a central biochemical mediator in responses to trauma. It has gained attention as a therapeutic target to modulate post-trauma symptoms and increase survival rates (22). Studies have found that excessive and prolonged circulating levels of IL-6 have decreased survival rate (23, 24), and progressive decline of IL-6 levels after three days of initial burn increases the chance of recovery in severely burn patients (25). Although it is still unclear where the excess IL-6 is produced, Chang and co-workers have suggested that the production of IL-6 is influenced by some factors released in the local burn tissue (26).

Modifying the inflammatory microenvironment through modulation of these cytokines, or the resultant activated immune cells, is therefore an appealing therapeutic strategy to rescue viable tissue from burn pathogenesis. In a rat model, topical application of inhibitor of p38MAPK, a potent stimulator of pro-inflammatory cytokine production and promoter of apoptosis, on burn injuries has shown significant reduction of local TNF-α, IL-1β, and IL-6 expression, attenuation of dermal neutrophil sequestration, and a lower level of hair follicle cell apoptosis within 24 hours of the initial burn injury (27). Intravenous injection of semapimod, a selective inhibitor of macrophage activation, one hour after burn in a swine model reduced depth of cellular necrosis and thrombosis, resulting in faster re-epithelialization (28). These studies have successfully demonstrated early intervention of inflammatory modulation can potentially halt burn wound progression, but developing a targeted method for accomplishing this without significant risks of systemic complications has not been achieved.

In order to achieve targeted modulation of the inflammatory microenvironment, we have conjugated TNF-α or IL-6 neutralizing antibodies with high molecular weight hyaluronic acid (HA), and applied these materials topically in a rat deep partial-thickness burn model. Rats were chosen for this study because it was possible to obtain commercial rat anti-mouse antibodies that are species-matched, avoiding potential complications associated with immunological responses to unmatched antibodies (29). These cytokines were targeted because of their established importance in burn etiology, and antibody conjugation to high molecular weight polysaccharides provides a means for inhibiting inflammatory responses at the site of injury (30). HA has been shown to promote wound healing in chronic wounds and other compromised tissues (31), and synergistic effects with cytokine-neutralizing antibodies may be anticipated. In this study, we compared the effects of locally inhibiting TNF-α, a potent upstream promoter of inflammation, with inhibiting IL-6, a downstream mediator of inflammation that is known to be important in burn etiology but has a range of functions bridging pro- and anti-inflammatory responses. The hypothesis of this study was that localized neutralization of TNF-α, an early mediator of inflammation, would be more effective at inhibiting burn progression than localized neutralization of IL-6, a late mediator of inflammation.

MATERIALS AND METHODS

Materials

Hyaluronic acid (HA, M_w = 1.6 MDa) and 4-(dimethylamino)pyridine (4-DMAP) were purchased from Sigma-Aldrich (St. Louis, MO) and used as received. *N*-hydroxysulfosuccinimide sodium salt (sulfo-NHS) and *N*-(3-dimethylaminopropyl)-*N*′-ethylcarbodiimide hydrochloride (EDC) were purchased from Pierce (Rockford, IL). Anti-rTNF-α and anti-rIL-6, both from purified mouse monoclonal IgG, were purchased from R&D Systems, Inc. (Minneapolis, MN). All reagents were reconstituted and stored according to the manufacturer's instructions.

Monoclonal antibody conjugation to HA

The conjugation chemistry followed a method previously developed in our laboratory. Briefly, HA (12 mg) was modified with an active ester group, followed by addition of anti-rTNF-α or anti-rIL6 mAb (1 mg), as shown in figure 1. The coupling reaction proceeded at 4 °C overnight. The product was dialyzed (MW cut-off 300 kDa, Next Group, Southborough, MA) against pure PBS for 24 hours with 4 changes of PBS solution at 4 °C. The final product consisted of roughly 1% (w/v) HA solution. In order to achieve a higher viscosity of solution that is more suitable for open wound applications, conjugate solution was made to contain 5% HA by mixing 3 parts of the conjugate product with 4 parts of 8% HA solution, and the final concentration of the cytokine-neutralizing antibody is roughly 400 μg/mL. A control of 5% HA solution was also prepared.

Rat deep partial-thickness burn model

All animal experiments were performed following the policies and procedures of the Institutional Animal Care and Use Committee at Institute of Surgical Research, Fort Sam Houston, TX. Rats received a single partial-thickness burn, treated with saline solution, HA, (anti-TNF-α)-HA, or (anti-IL-6)-HA (N=4 for all treatments). The rats were anesthetized throughout the procedures and all subsequent treatments and dressing changes. Buprenorphine was given as pre-emptive analgesia (0.1–0.2mg/kg IP or SQ) and isoflurane (2%–5% in O_2 via facemask) given to effect anesthesia. Buprenorphine (0.1 to 0.2mg/kg) was provided at 12 hours and 24 hours post-surgery and continued as necessary upon the observation of signs of continued pain based on clinical assessment, using the pain/distress assessment scoring sheets.

A commercially available soldering unit was used as a controlled heat source. The soldering iron was modified by welding a 17 mm diameter, 2.5 mm thick brass disk on the tip and weighted with 500 g to induce sufficient pressure for efficient heat transfer. The non-contacting side of the disc was connected to a thermal coupler to monitor the actual temperature of the disk, as shown in figure 2A. Burn injuries were induced on the back of shaved, anesthetized adult male Sprague-Dawley rats with masses ranging from 230–250 g (N=4). The brass disc was heated to 85 °C, stabilized for 2 min, and the burn injury inflicted by placing the brass disc on the skin for 10 s.

Consistency of wound depth was assessed in separate preliminary experiments using collagen IV immunostaining to verify the reproducibility of deep partial-thickness burns at the sites (data not shown) (1). Eschar was surgically removed following the circumference of the non-viable tissue the next day using surgical scissors taking extreme care to only debride the necrotic tissue and not cause further injury, and was done blinded to the treatment specification until after the procedure was complete. Surgical debridement is a very common technique in burn wound care to prevent infection and aid healing because it is simple and selective. Burn depth was visually assessed after eschar removal to ensure the consistency of the injury. The viable tissue underneath was exposed and the treatments were applied immediately after. The procedure is shown in figure 2B-2E.

Rats were randomized for different treatments and different time points. Eschar removal date was defined as day 0, at which point the first 200 μL treatment was applied. The wounds were dressed with commercially available Tegaderm™ and sealed with Vetbond (3M, St. Paul, MN), and remained moist throughout the experiments with no further loss of tissue observed in dressing changes. Treatments were applied at day 0, 2 and 4 and rats were euthanized on days 1, 4 or 7 providing tissue samples from rats that received 1, 2 or 3 treatments, respectively. The tissues were sectioned into three: one was fixed with 10% formaldehyde for histology analysis, another was flash frozen in tissue embedding media for further sectioning and immunohistochemistry, and the other was stored in RNAlater solution (Ambion, Austin, TX) at 4 °C overnight, followed by long-term storage at −80 °C.

Extraction of tissue cytokines

The RNAlater-preserved tissues were cut into approximately 0.1 g pieces that were then homogenized in 600 μL of T-PER Tissue Protein Extraction solution (Thermo Scientific, Rockford, Illinois), a mild detergent, for total protein extraction. Homogenates were centrifuged at 10,000 rcf for 5 min to remove large tissue particles. The resulting supernatant was removed and stored at −80 °C.

Total protein and ELISA assays from burn tissue

The supernatants were thawed and quantitatively assayed for total protein concentrations using the Pierce BCA Protein Assay kit (Thermo Scientific, Rockford, Illinois). For this assay, samples were diluted 1:20 in PBS. The assay was carried out according to the kit's procedure with a 1:8 ratio of diluted sample to BCA working reagent and analyzed by SAFIRE microplate reader (SAFIRE, San Jose, CA) with absorbance set at 562 nm. ELISA assays for IL-1β concentrations from tissue extracts were done using the respective Quantikine Rat ELISA kits (R&D Systems, Minneapolis, MN) using a 96-well plate reader. Assay samples for IL-1β were diluted according to procedure at dilutions of 1:10. All assays were done according to the kit procedures and analyzed at 562 nm with a 549 nm correction. The resulting total protein and cytokine concentrations were verified by using internal controls with a known concentration of the target protein, supplied with each kit. Curve fitting to the standards was used to express the concentration of both total protein and cytokines in the tissue samples in pg/mg protein.

Histological and immunohistochemical staining

The explanted burn site specimens were mounted on glass slides and embedded in paraffin, then subsequently deparaffinized with xylene followed by a graded series of ethanol solutions (100–70%). Sections were then stained with Masson's Trichrome using a microwave staining protocol (Richard-Allen Scientific, Kalamazoo, MI) for morphological assessment. The slides were then cleared and dehydrated using the reverse of the deparaffinization treatment described above prior to coverslip mounting. Following deparaffinization, the slides were immersed in citrate antigen retrieval buffer (10 mM citric acid monohydrate, pH 6.0, Spectrum, Gardena, CA) that was then brought to a boil (95–100 °C) for 20 min. The buffer was allowed to cool and the slides were then washed twice in TRIS-buffered saline-Tween 20 (Trizma Base, Tween 20, Sigma) solution (pH 7.4) and twice in PBS. The tissue sections were encircled with a hydrophobic barrier pen and were incubated in T20 blocking buffer (Pierce, Rockford, IL) for 1 hour at room temperature in a humidified chamber to inhibit nonspecific binding of the primary antibody. Following incubation in blocking serum, the sections were incubated in primary antibody, mouse anti-rat CD68 (Serotec, Raleigh, NC), diluted to 1:100 in PBS, in a humidified chamber at 4 °C overnight. Following the overnight incubation, the slides were washed three times in PBS. Sections were then incubated in a solution of 3% H_2O_2 in methanol for 20 min at room temperature to quench endogenous peroxidase activity. The slides were washed three times in PBS before incubation in secondary antibody, biotinylated horse anti-mouse IgG (Vector, Burlingame, CA), diluted 1:150 in PBS for 1 hour in a humidified chamber at room temperature, and then subjected to three more washes in PBS. The sections were then incubated in Vectastain ABC (Elite ABC kit, Vector) reagent for 30 min in a humidified 37 °C chamber, again rinsed three times in PBS, and incubated in 4% diaminobenzadine substrate solution (DAB substrate peroxide kit, Vector) at room temperature. The slides were rinsed in water to stop the development of the diaminobenzadine substrate and counterstained using Harris hematoxylin stain (Vector). The slides were then dehydrated using the reverse of the deparaffinization treatment described above prior to cover slipping. Each PBS rinse in the protocol was for 3 min at room temperature, with occasional agitation.

Immunohistochemical analysis

The immunostained slides were examined and imaged using a Leica DM IL LED microscope (Germany). The CD68 stained images were then evaluated quantitatively in a blinded fashion by two independent investigators (MR and JP). Quantitative analysis was performed by counting the number of immunopositive cells in three matched microscope fields at 20x magnification. The number of positive stained cells was then averaged to obtain the final results. The vimentin-stained images were quantified in two separate rounds of blinded analysis, and the average thickness of the necrotic tissue was measured at three different regions of the burn wounds: the two edges and the center. The measurements were then averaged for the final results.

Statistical Analysis

One-way ANOVA were performed for ELISA, vimentin measurements and macrophage counts using Minitab statistical software. Data were log transformed in order to pass a normality test for ELISA and vimentin measurements. The Dunnet and Tukey's methods were used as the post tests to determine which groups were significantly different from saline control and from each other respectively.

RESULTS

Evaluation of trichrome staining: gross appearance of the burn site

Trichrome images of the burn tissue treated with saline, HA, (anti-IL-6)-HA, and (anti-TNF-α)-HA were examined to evaluate gross appearance of the wound and the effect of treatments on the healing progression, as shown in figure 3. The apical surface of the wound bed was created by eschar removal 1 day following primary injury. Newly formed granulation tissue started to appear underneath the intact dermis, and significant amounts of granulation tissue were observed in (anti-TNF-α)-HA treated wounds on day 7. A unique layer of tissue, stained in red, can be identified above the wound edges at later time points. This intensely stained layer of tissue, which was postulated to be the dermal tissue that had undergone secondary necrosis after burn, grew significantly under most of the treatments, shown on the day 7 images, except (anti-TNF-α)-HA treatment group. In spite of the growing necrosis, granulation tissues occupied most of the defect zone in HA-treated burn wounds, while saline- and (anti-IL-6)-HA-treated wounds have shown less granulation tissue formation.

Vimentin immunohistochemistry and necrotic tissue quantification

In order to investigate further the extent of necrosis, vimentin immunostaining was utilized to visualize viable tissues, and non-stained regions were identified as necrotic. Vimentin is a cytoskeletal protein that Nanney and co-workers established as a marker for viable tissue at burn sites (33). In figure 4, a dashed line was carefully drawn in each image to indicate the approximate separation of healthy dermis and nonviable tissue. There was no visual evidence of necrosis in the images of day 1 samples, due to the eschar removal the day before. However, the growing depth of nonviable tissues is clearly observable in the images of day 4 and day 7 in all treatment groups, except (anti-TNF-α)-HA.

The thickness of necrotic tissue was measured manually by two personnel on blinded samples, and average thickness of three different locations, two on each of the edges and one on the center of the burn, on each tissue slide was reported. On day 7, the difference in thickness of necrotic zones from (anti-TNF-α)-HA treated group was significantly lower than in any other group ($p=.001$).

Tissue cytokine concentration

Proteins in the local burn tissue were extracted from RNAlater-preserved tissue. ELISA assays were performed to measure the tissue concentration of IL-1β in pg/mL, which was then converted to pg IL-1β/mg total protein. IL-1β is centrally involved in inflammatory responses, making it a good marker for the overall state of inflammation following burn injury (34). Measured IL-1β concentrations are shown in figure 6. IL-1β expression was significantly suppressed by (anti-TNF-α)-HA treatments compared to saline on day 4 ($p<0.05$) and day 7 ($p<0.05$). IL-1β concentrations trend lower in (anti-TNF-α)-HA treated burn wounds compared to HA treatment on day 4 and 7 as well, with HA treatments also showing a trend towards decreased IL-1β levels compared to saline only on day 1. However, (anti-IL-6)-HA treatments did not have significant effect on IL-1β expression, beyond a less robust and non-significant decrease compared to saline on days 1 and 4, suggesting that neutralization of IL-6 had little effect on the overall inflammatory microenvironment.

Macrophage infiltration

In order to investigate further the anti-inflammatory effects of the cytokine-neutralizing HA conjugates, paraffin-embedded tissue sections were stained for a pan-macrophage marker, CD68 (30). High-power images (20x) were taken at the subcutaneous regions at the wound edges, shown in figure 7, and the numbers of positively stained cells and non-stained cells

were counted in a blinded manner by three independent personnel. The results from quantification are shown in figure 7E. (Anti-TNF-α)-HA treated wound sites have clearly demonstrated a reduction of macrophage numbers throughout the experimental duration. (Day 1:$p<0.001$, Day 4: $p<0.05$, Day 7: $p=0.005$) Interestingly, HA-treated sites did not have measurably different numbers of CD68+ cells compared to saline treatment. This contrasts with the results observed in treatment of incisional wounds with HA, for which we observed a significant increase in numbers of recruited macrophages (30). In addition, (anti-IL-6)-HA treated injury sites did not demonstrate any observable effect on the number of CD68+ cells at the burn site, suggesting neutralization of this cytokine did little to reduce the state of inflammation at burn sites.

DISCUSSION

In this research, we compared the effects of locally inhibiting TNF-α and IL-6 in a rat partial-thickness burn model, and the results indicate that modulating the activities of a cytokine at the apex of the signaling cascade (TNF-α) was more effective in reducing necrosis than targeting a downstream mediator (IL-6) in the context of burn wound healing.

There are conflicting reports on the levels of TNF-α following burns, primarily because the baseline serum levels in healthy patients are low (< 1 pg/mL) and only increase by a factor of 5 in the first week following burns (21). Nevertheless, it is known that TNF-α is a potent stimulator of inflammation and occupies a central position in the inflammatory cascade, being among the first inflammatory response molecules to be upregulated following injury and stimulating the production of numerous downstream mediators that are measured in burn sites (36). Some of the most successful drugs currently marketed are based on TNF-α inhibition (35) and are used to treat a broad range of inflammatory conditions, such as psoriasis, rheumatoid arthritis, and inflammatory bowel disease. That each of these widely varying disease states can be treated through inhibition of the same signaling protein speaks to the fundamental importance of TNF-α in inflammatory processes. Effects of mediating inflammation in a burn wounds, specifically through local TNF-α inhibition, have yet to be thoroughly explored. Our data support a first insight into yet another disease state that can potentially be treated through inhibition of TNF-α.

In contrast to TNF-α, IL-6 increases measurably in burn patients (34). Signaling by IL-6 can support inflammatory responses, such as recruitment of mononuclear cells, and inhibition of T-cell apoptosis and T_{reg} differentiation (37). It is also known to play a central role in anti-inflammatory signaling, in some settings even inhibiting TNF-α (19, 38) and stimulating interleukin-1 receptor antagonist and interleukin-10 production (39, 40). It is further downstream in the signaling cascade and thought to be a bridge between inflammation and healing. The pleiotropic nature of IL-6 may provide only a small therapeutic window to which inhibition of the cytokine would produce an effective anti-inflammatory effect. In light of this, it may not be surprising that we saw no measurable effect in IL-1β levels and amounts of necrotic tissue in (anti-IL-6)-HA treated wounds.

Pathogenic inflammation leads to increased blood vessel permeability and increased levels of blood vessel damaging ROS (22, 41). Degeneration of blood vessels and capillaries occurs through several mechanisms in burn wound etiology related to proinflammatory mediators such as TNF-α and IL-6 (4, 42). TNF-α is considered to be a more potent pro-inflammatory cytokine than IL-6, though, and is capable of inducing a wide variety of factors that leads to subsequent pathology. This was observed histologically, where blood vessels had a dramatically different visual appearance after injury, suggesting these are signs of vasodilation or blood clots. Furthermore, damage to blood vessels appeared to be minimized by the treatment with (anti-TNF-α)-HA but not by (anti-IL-6)-HA.

Cellular contributions to wound progression include neutrophil and macrophage dysfunctions. Neutrophils are attracted to the injury site with increasing expression of adhesion molecules stimulated by pro-inflammatory cytokines and abundant chemotactic signals in the wound (43). Macrophages are hyperactivated post-burn, and release a host of pro-inflammatory mediators, which also have been suggested to lead to the down-stream immune-suppression state (44, 45). Several studies have differentially inhibited the interaction between cell-adhesion molecules and integrins and demonstrated that minimizing neutrophil and macrophage infiltration reduces wound progression (46, 47). TNF-α is a potent activator of endothelial cells to induce expression of cell adhesion molecules, and modulating the activities of TNF-α has shown to decrease macrophage infiltration (30), which supports our data indicating lower CD68 macrophage counts in (anti-TNF-α)-HA treated rats.

As previously mentioned, modulating acute inflammation using p38MAPK inhibitor was shown to be effective in reducing cellular apoptosis (27), but the long-term effect of such treatment was unclear. Singer and co-workers have also demonstrated 30% reduction in depth of hair follicle necrosis after systemic delivery of semapimod in a pig model (28), while systemic delivery of curcumin has shown a positive effect in reducing burn wound progression by 50% in a rat comb burn model seven days after initial burn (48). However, systemic delivery of anti-inflammatory agents in a burn patient increases the risk of secondary complications, and local delivery of TNF-α neutralizing agent from a hyaluronic acid delivery vehicle has reduced necrosis by up to 70% post burn in a rat model. In addition to providing a means of local delivery, we believe there may be synergistic effects on healing between hyaluronic acid, the degradation products of which are known to function as damage-associated molecular patterns and the TNF-α antibody. This will be explored further in subsequent studies.

Localized neutralization of TNF-α with antibody-polysaccharide conjugates is an appealing strategy for locally controlling the inflammatory processes associated with burn progression. Our results suggest that inhibition of a central, upstream mediator of inflammation is more effective than downstream cytokines, such as IL-6. The doses used in these studies followed the antibody doses used in our previous study on reducing inflammation in incisional wounds (30). While many of the systemic side-effects associated with TNF-α inhibitors can be avoided with this approach, there is still clearly an increased risk for infection at injury sites, although none have been observed in either incisional or burn studies thus far. Understanding the dose-response behavior at a fundamental level will be critical for evaluating the potential clinical efficacy of these materials.

Acknowledgments

The authors acknowledge support from the Armed Forces Institute of Regenerative Medicine (W81XWH-08-2-0032) and the National Institutes of Health (R43GM085897). NRW gratefully acknowledges support from a 3M Non-Tenured Faculty Grant, the Wallace H. Coulter Foundation Translational Research Award program, and the Heinz Endowment (C1747). REP and NMD wish to thank the Howard Hughes Medical Institute for support through the Undergraduate Science Education Program at CMU (52005865). The authors also wish to thank Dr. Yoram Vodovotz and Dr. Lillian Nanney for helpful discussions and John Walters for help with statistical analysis.

References

1. Jackson DM. The diagnosis of the depth of burning. Br J Surg. 1953; 40(164):588–96. [PubMed: 13059343]
2. Gravante G, Palmieri MB, Esposito G, Delogu D, Santeusanio G, Filingeri V, Montone A. Apoptotic death in deep partial thickness burns vs. normal skin of burned patients. J Surg Res. 2007; 141:141–5. [PubMed: 17559878]

3. Gravante G, Filingeri V, Delogu D, Santeusanio G, Palmieri MB, Esposito G, Montone A, Sconocchia G. Apoptotic cell death in deep partial thickness burns by coexpression analysis of TUNEL and Fas. Surgery. 2006; 139:854–5. [PubMed: 16782446]

4. Singh V, Devgan L, Bhat S, Milner SM. The pathogenesis of burn wound conversion. Ann Plast Surg. 2007; 59:109–15. [PubMed: 17589272]

5. Kao CC, Garner WL. Acute Burns. Plast Reconstr Surg. 2000; 101:2482–93. [PubMed: 11242345]

6. Arturson G. Pathophysiology of the burn wound and pharmacological treatment. The Rudi Hermans Lecture, 1995 Burns. 1996; 22:255–74.

7. Shupp JW, Nasabzadeh TJ, Rosenthal DS, Jordan MH, Fidler P, Jeng JC. A review of the local pathophysiologic bases of burn wound progression. J Burn Care Res. 2010; 31:849–73. [PubMed: 21105319]

8. Piguet PF, Grau GE, Vassalli P. Tumor necrosis factor and immunopathology. Immunol Res. 1991; 10:122–40. [PubMed: 1717618]

9. Diegelmann RF, Evans MC. Wound healing: an overview of acute, fibrotic and delayed healing. Front Biosci. 2004; 9:283–9. [PubMed: 14766366]

10. Horton JW. Free radicals and lipid peroxidation mediated injury in burn trauma: the role of antioxidant therapy. Toxicology. 2003; 189:75–88. [PubMed: 12821284]

11. Young CN, Koepke JI, Terlecky LJ, Borkin MS, Boyd Savoy L, Terlecky SR. Reactiv oxygen species in tumor necrosis factor-alpha-activated primary human keratinocytes: implications for psoriasis and inflammatory skin disease. J Invest Dermatol. 2008; 128:2606–14. [PubMed: 18463678]

12. Camacho M, Lopez-Belmonte J, Vila L. Rate of vasoconstrictor prostanoids released by endothelial cells depends on cyclooxygenase-2 expression and prostaglandin I synthase activity. Circ Res. 1998; 83:353–65. [PubMed: 9721692]

13. Koide M, Kawahara Y, Tsuda T, Yokoyama M. Cytokine-induced expression of an inducible type of nitric oxide synthase gene in cultured vascular smooth muscle cells. FEBS Lett. 1993; 318:213–7. [PubMed: 7680009]

14. O'Neill LA, Lewis GP. Interleukin-1 potentiates bradykinin- and TNF alpha-induced PGE2 release. Eur J Pharmacol. 1989; 166:131–7. [PubMed: 2507329]

15. Gao X, Xu X, Belmadani S, Park Y, Tang Z, Feldman AM, Chilian WM, Zhang C. TNF-alpha contributes to endothelial dysfunction by upregulating arginase in ischemia/reperfusion injury. Arterioscler Thromb Vasc Biol. 2007; 27:1269–75. [PubMed: 17413034]

16. Johns DG, Webb RC. TNF-alpha-induced endothelium-independent vasodilation: a role for phospholipase A2-dependent ceramide signaling. Am J Physiol. 1998; 275:H1592–8. [PubMed: 9815065]

17. Zhang C, Xu X, Potter BJ, Wang W, Kuo L, Michael L, Bagby GJ, Chilian WM. TNF-alpha contributes to endothelial dysfunction in ischemia/reperfusion injury. Arterioscler Thromb Vasc Biol. 2006; 26:475–80. [PubMed: 16385082]

18. Kishimoto T. The biology of interleukin-6. Blood. 1989; 74:1–10. [PubMed: 2473791]

19. Schindler R, Mancilla J, Endres S, Ghorbani R, Clark SC, Dinarello CA. Correlations and interactions in the production of interleukin-6 (IL-6), IL-1, and tumor necrosis factor (TNF) in human blood mononuclear cells: IL-6 suppresses IL-1 and TNF. Blood. 1990; 75:40–7. [PubMed: 2294996]

20. Nishimoto N, Kishimoto T. Interleukin 6: from bench to bedside. Nat Clin Pract Rheumatol. 2006; 2:619–26. [PubMed: 17075601]

21. Finnerty CC, Herndon DN, Przkora R, Pereira CT, Oliveira HM, Queiroz DM, Rocha AM, Jeschke MG. Cytokine expression profile over time in severely burned pediatric patients. Shock. 2006; 26:13–9. [PubMed: 16783192]

22. Biffl WL, Moore EE, Moore FA, Peterson VM. Interleukin-6 in the injured patient. Marker of injury or mediator of inflammation? Ann Surg. 1996; 224:647–64. [PubMed: 8916880]

23. Guo Y, Dickerson C, Chrest FJ, Adler WH, Munster AM, Winchurch RA. Increased levels of circulating interleukin 6 in burn patients. Clin Immunol Immunopathol. 1990; 54:361–71. [PubMed: 2406054]

24. Drost AC, Burleson DG, Cioffi WG Jr, Mason AD Jr, Pruitt BA Jr. Plasma cytokines after thermal injury and their relationship to infection. Ann Surg. 1993; 218:74–8. [PubMed: 8328832]
25. Schluter B, Konig B, Bergmann U, Muller FE, Konig W. Interleukin 6--a potential mediator of lethal sepsis after major thermal trauma: evidence for increased IL-6 production by peripheral blood mononuclear cells. J Trauma. 1991; 31:1663–70. [PubMed: 1749040]
26. Chang KC, Ma H, Liao WC, Lee CK, Lin CY, Chen CC. The optimal time for early burn wound excision to reduce pro-inflammatory cytokine production in a murine burn injury model. Burns. 2010; 36:1059–66. [PubMed: 20471756]
27. Ipaktchi K, Mattar A, Niederbichler AD, Hoesel LM, Hemmila MR, Su GL, Remick DG, Wang SC, Arbabi S. Topical p38MAPK inhibition reduces dermal inflammation and epithelial apoptosis in burn wounds. Shock. 2006; 26:201–9. [PubMed: 16878030]
28. Singer AJ, McClain SA, Hacht G, Batchkina G, Simon M. Semapimod reduces the depth of injury resulting in enhanced re-epithelialization of partial-thickness burns in swine. J Burn Care Res. 2006; 27:40–9. [PubMed: 16566536]
29. Khazaeli MB, Conry RM, LoBuglio AF. Human immune response to monoclonal antibodies. J Immunother Emphasis Tumor Immunol. 1994; 15:42–52. [PubMed: 8110730]
30. Sun LT, Bencherif SA, Gilbert TW, Farkas AM, Lotze MT, Washburn NR. Biological activities of cytokine-neutralizing hyaluronic acid-antibody conjugates. Wound Repair Regen. 2010; 18:302–10. [PubMed: 20412551]
31. Steed DL, Ricotta JJ, Prendergast JJ, Kaplan RJ, Webster MW, McGill JB, Schwartz SL. Promotion and acceleration of diabetic ulcer healing by arginine-glycine-aspartic acid (RGD) peptide matrix. RGD Study Group. Diabetes Care. 1995; 18:39–46. [PubMed: 7698046]
32. Ho-Asjoe M, Chronnell CM, Frame JD, Leigh IM, Carver N. Immunohistochemical analysis of burn depth. J Burn Care Rehabil. 1999; 20:207–11. [PubMed: 10342472]
33. Nanney LB, Wenczak BA, Lynch JB. Progressive burn injury documented with vimentin immunostaining. J Burn Care Rehabil. 1996; 17:191–8. [PubMed: 8736363]
34. Finnerty CC, Przkora R, Herndon DN, Jeschke MG. Cytokine expression profile over time in burned mice. Cytokine. 2009; 45:20–5. [PubMed: 19019696]
35. Ackermann C, Kavanaugh A. Tumor necrosis factor as a therapeutic target of rheumatologic disease. Expert Opin Ther Targets. 2007; 11:1369–84. [PubMed: 18028004]
36. Duan H, Chai J, Sheng Z, Yao Y, Yin H, Liang L, Shen C, Lin J. Effect of burn injury on apoptosis and expression of apoptosis-related genes/proteins in skeletal muscles of rats. Apoptosis. 2009; 14:52–65. [PubMed: 19009350]
37. Scheller J, Chalaris A, Schmidt-Arras D, Rose-John S. The pro- and anti-inflammatory properties of the cytokine interleukin-6. Acta Biochim Biophys Sin. 2011; 1813:878–88.
38. Starkie R, Ostrowski SR, Jauffred S, Febbraio M, Pedersen BK. Exercise and IL-6 infusion inhibit endotoxin-induced TNF-alpha production in humans. FASEB J. 2003; 17:884–6. [PubMed: 12626436]
39. Tilg H, Trehu E, Atkins MB, Dinarello CA, Mier JW. Interleukin-6 (IL-6) as an anti-inflammatory cytokine: induction of circulating IL-1 receptor antagonist and soluble tumor necrosis factor receptor p55. Blood. 1994; 83:113–8. [PubMed: 8274730]
40. Steensberg A, Fischer CP, Keller C, Moller K, Pedersen BK. IL-6 enhances plasma IL-1ra, IL-10, and cortisol in humans. Am J Physiol Endocrinol Metab. 2003; 285:E433–7. [PubMed: 12857678]
41. Maruo N, Morita I, Shirao M, Murota S. IL-6 increases endothelial permeability in vitro. Endocrinology. 1992; 131:710–4. [PubMed: 1639018]
42. Leach L, Eaton BM, Westcott ED, Firth JA. Effect of histamine on endothelial permeability and structure and adhesion molecules of the paracellular junctions of perfused human placental microvessels. Microvasc Res. 1995; 50:323–37. [PubMed: 8583948]
43. Calum H, Moser C, Jensen PO, Christophersen L, Maling DS, van Gennip M, Bjarnsholt T, Hougen HP, Givskov M, Jacobsen GK, Hoiby N. Thermal injury induces impaired function in polymorphonuclear neutrophil granulocytes and reduced control of burn wound infection. Clin Exp Immunol. 2009; 156:102–10. [PubMed: 19210518]
44. Schwacha MG. Macrophages and post-burn immune dysfunction. Burns. 2003; 29:1–14. [PubMed: 12543039]

45. Schwacha MG, Schneider CP, Bland KI, Chaudry IH. Resistance of macrophages to the suppressive effect of interleukin-10 following thermal injury. Am J Physiol Cell Physiol. 2001; 281:C1180–7. [PubMed: 11546654]

46. Bucky LP, Vedder NB, Hong HZ, Ehrlich HP, Winn RK, Harlan JM, May JW Jr. Reduction of burn injury by inhibiting CD18-mediated leukocyte adherence in rabbits. Plast Reconstr Surg. 1994; 93:1473–80. [PubMed: 7911582]

47. Hansbrough JF, Wikstrom T, Braide M, Tenenhaus M, Rennekampff OH, Kiessig V, Zapata-Sirvent R, Bjursten LM. Effects of E-selectin and P-selectin blockade on neutrophil sequestration in tissues and neutrophil oxidative burst in burned rats. Crit Care Med. 1996; 24:1366–72. [PubMed: 8706493]

48. Singer AJ, Taira BR, Lin F, Lim T, Anderson R, McClain SA, Clark RA. Curcumin reduces injury progression in a rat comb burn model. J Burn Care Res. 2011; 32:135–42. [PubMed: 21088615]

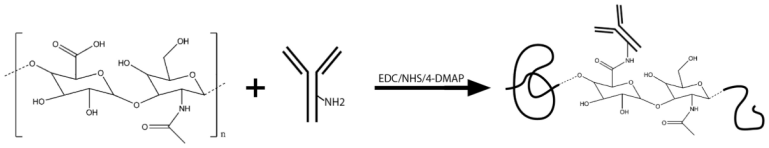

Figure 1.
Synthesis of (anti-TNF-α)-HA and (anti-IL-6)-HA conjugates. Carboxylic acid groups on HA were partially activated followed by coupling reaction with the amine groups on cytokine-neutralizing monoclonal antibodies.

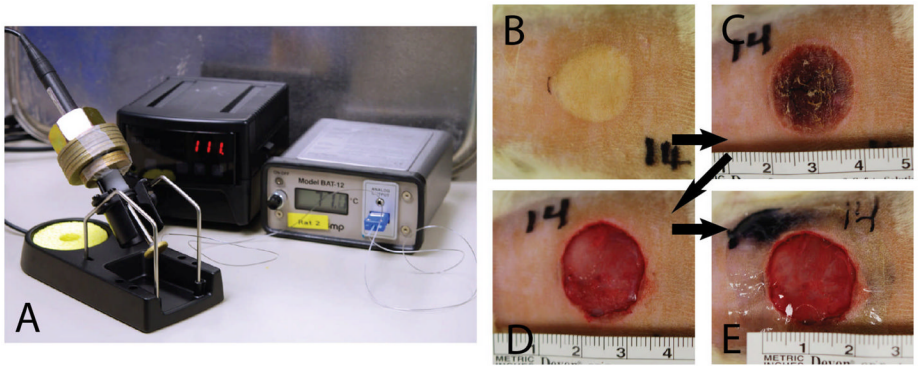

Figure 2.

Rat partial thickness contact burn model. (A) The burn unit was assembled with a modified soldering unit that provided heat energy for a Ø17mm brass disk. In order to provide consistent pressure against skin, the burn unit was weighted 500 g, and the brass disk was connected to a thermometer to monitor the actual temperature of the unit. (B) A representative image of a shaved rat skin that just underwent 10 second of contact with an 85°C brass disk. (C) After 24 hours, the burn area has developed into an eschar. (D) The eschar was surgically removed and the underlying skin tissue was exposed. (E) Treatments were applied and the wounds were dressed with Tegaderm™ (3M).

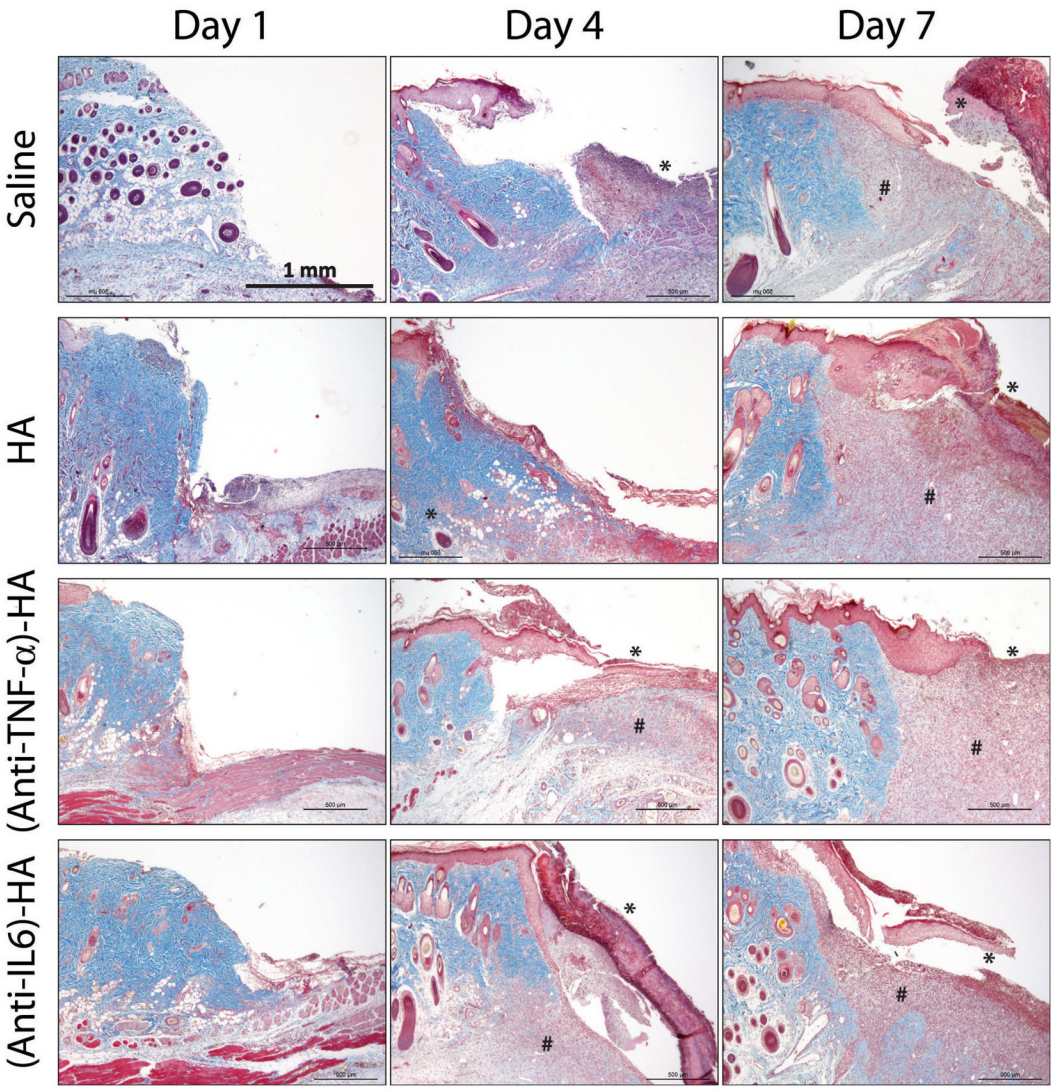

Figure 3.

Masson's trichrome images of the edges of the burn site arranged according to treatments and time points. All images are at 4x magnification. Clear excision lines are present in the day 1 images, and some evidence of microthrombosis caused by the initial burn is visible, especially in images of saline controls. Granulation tissues start to appear four days after eschar removal in the deep dermal region. By day 7, granulation tissue has grown to fill most of the defect space in HA and (anti-TNF-α)-HA treated sites, while saline and (anti-IL-6)-HA treated wound sites seem to display slower granulation tissue formation. On day 4, a layer of necrotic tissue on the surface of the wounds is observed in most of the wound sites, and on day 7, necrosis has grown significantly particularly in saline, HA, and (anti-IL-6)-HA treated burn sites. In several instances this layer of necrosis is separated from the underlying healthy tissue during histology process. (* = necrosis, and # = granulation tissue)

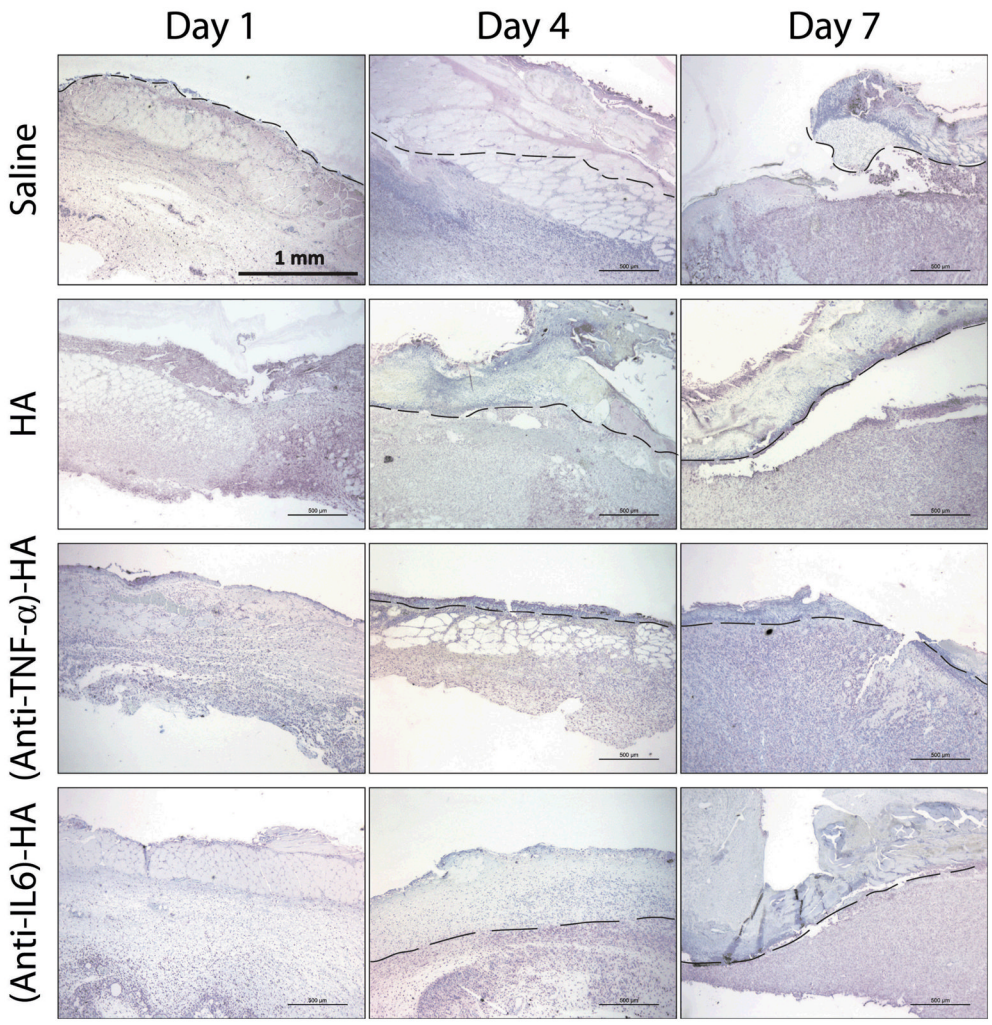

Figure 4.
Vimentin IHC stained (pink) burn wound images at 4x magnification arranged according to treatments and time points. Dashed lines represents the separation of necrosis and viable tissue. On day 1, there is no visible evidence of necrosis, due to the excision of eschar the day before. On day 4, a layer of non-stained tissue is observed, suggesting that wound progression has penetrated into deeper layer of skin. On day 7, the size of the necrosis is significantly smaller in (anti-TNF-α)-HA treated wound sites than that under other treatments.

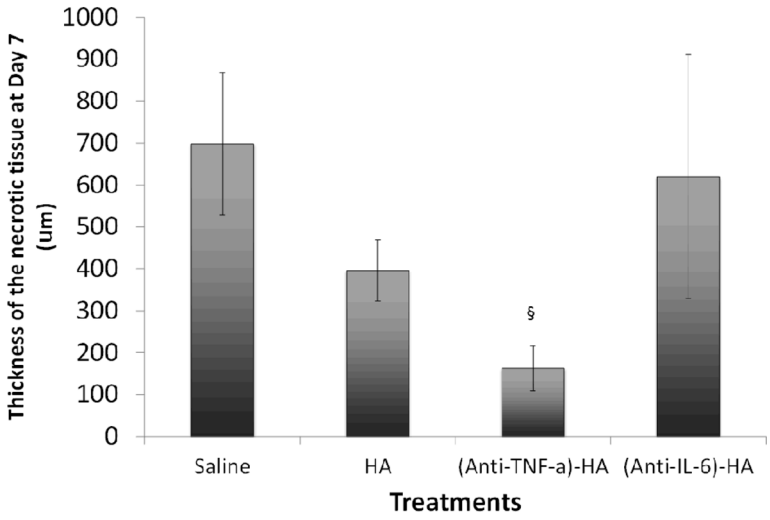

Figure 5.

Thickness of necrotic tissue on day 7. (Anti-TNF-α)-HA treated burn sites have significantly thinner necrotic zones than the other compositions treated sites. HA treatment also appears to reduce necrotic conversion comparing to saline treated controls. (§: $p<0.001$)

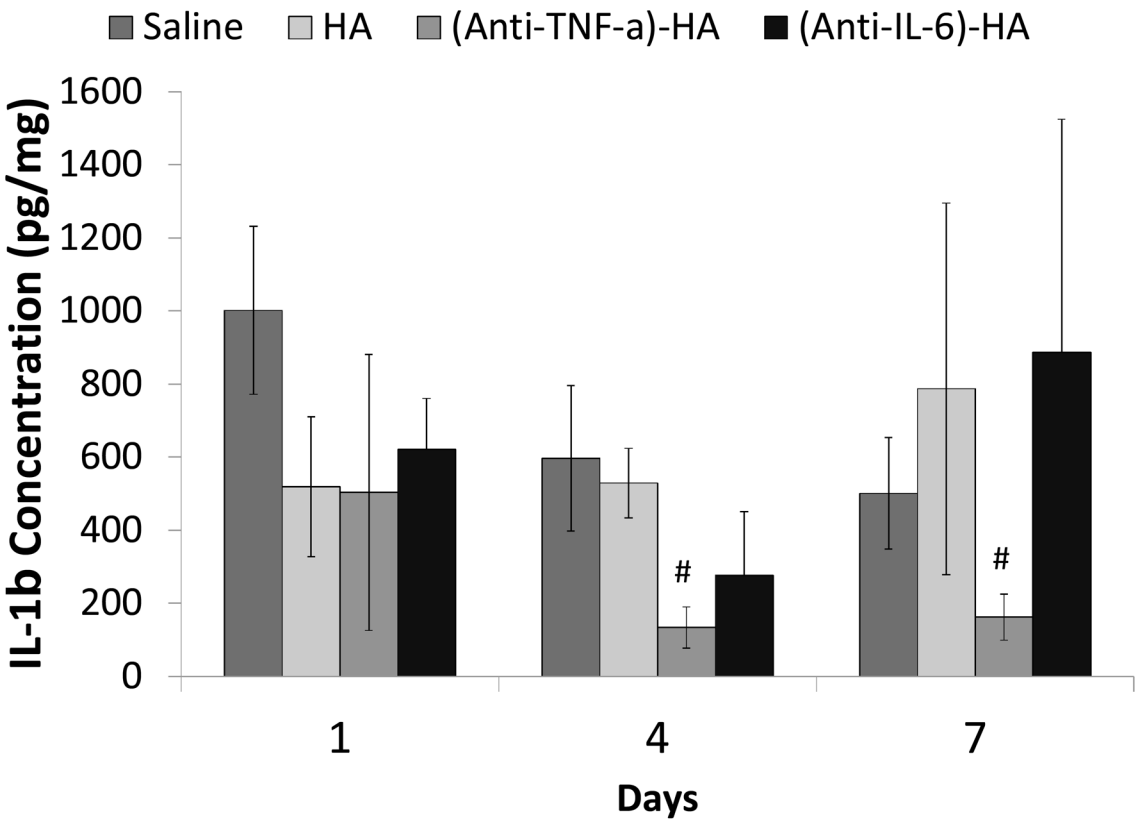

Figure 6.

IL-1β concentration in the local burn tissue. IL-1β concentration peaks at day 1, and attenuate on day 4 in saline treated controls. (Anti-TNF-α)-HA treated wound sites show similar trend of IL-1β response, while the IL-1β levels are significant lower than those in saline treated sites throughout the experimental period. HA initially inhibits the IL-1β expression on day 1, and the level of IL-1β is kept about the same level until the end of the experimental period, suggesting HA has limited effect in suppressing inflammation. (Anti-IL-6)-HA treated wounds sites demonstrats no specific trends to IL-1β expression. (#: $p<0.05$)

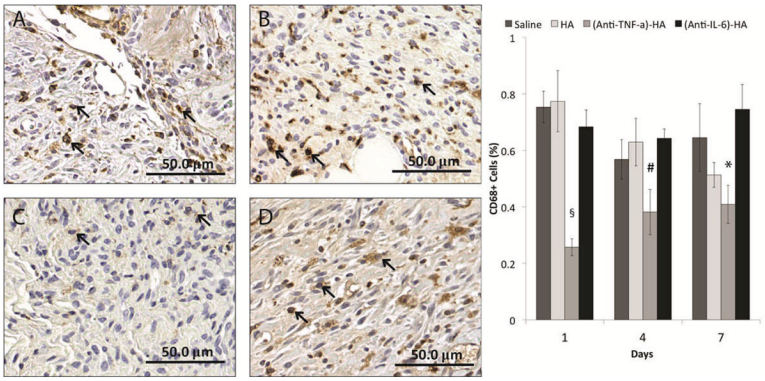

Figure 7.

CD68 IHC stained burn wound images of day 4 treated with (A) saline, (B) HA, (C) (anti-TNF-α)-HA, and (D) (anti-IL-6)-HA at 20x magnification and the result of CD68+ cell counts. The arrows indicates the positively stained cells, and (anti-TNF-α)-HA treated wounds exhibit gross reduction of CD68 staining, and the quantification result verifies the significant reduction of CD68+ cell numbers in (anti-TNF-α)-HA treatment comparing to all the other treatments at all three time points. HA treated wounds show monotonic decrease of CD68+ cells from day 1 to 7 without statistical significance. The other two treatments show high level of CD68+ cells throughout the experiments. (#: $p<0.05$, *: $p<0.005$, §: $p<0.001$)